Research Article

For reprint orders, please contact: reprints@futuremedicine.com

Nanomedicine

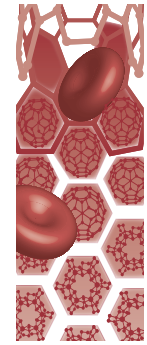

# Cholic acid-based novel micellar nanoplatform for delivering FDA-approved taxanes

**Aim:** To structurally modify our existing cholic acid (CA)-based telodendrimer (TD; $PEG^{5K}$-$CA_8$) for effective micellar nanoencapsulation and delivery of the US FDA-approved members of taxane family. **Materials & methods:** Generation of hybrid TDs was achieved by replacing four of the eight CAs with biocompatible organic moieties using solution-phase peptide synthesis. Drug loading was done using the standard evaporation method. **Results:** Hybrid TDs can generate micelles with narrow size distributions, low critical micelle concentration values (1–6 μM), better hematocompatibility and lack of *in vitro* cytotoxicity. **Conclusion:** Along with $PEG^{5K}$-$CA_8$, CA-based hybrid nanoplatform is the first of its kind that can stably encapsulate all three FDA-approved taxanes with nearly 100% efficiency up to 20% (w/w) loading.

First draft submitted: 12 October 2016; Accepted for publication: 6 March 2017; Published online: 27 April 2017

**Keywords:** cabazitaxel • cholic acid • docetaxel • drug delivery • micelle • nanoparticle • paclitaxel • taxane • telodendrimer

Gaurav Bharadwaj[1], Viet Nhan[1,2], ShanChao Yang[1], Xiaocen Li[1], Anand Narayanan[1], Ana Carolina Macarenco[1,3], Yu Shi[1,4], Darrion Yang[1], Letícia Salvador Vieira[1,3], Wenwu Xiao[1], Yuanpei Li[1] & Kit S Lam*[,1]

[1]Department of Biochemistry & Molecular Medicine, UC Davis Cancer Center, University of California Davis, Sacramento, CA 95817, USA
[2]Biology Department, California State University Channel Islands, Camarillo, CA 93012, USA
[3]School of Pharmaceutical Science of Ribeirão Preto, University of Sao Paulo, Ribeirão Preto 14040-903, Brazil
[4]Tianjin Institutes of Pharmaceutical Research Co., Ltd, Tianjin 300193, PR China
*Author for correspondence:
Tel.: +1 916 734 0910
Fax: +1 916 734 4418
kslam@ucdavis.edu

Taxanes are a benchmark class of small-molecule anticancer agents that work by interfering with normal microtubule breakdown during cell division [1–3]. Currently, three members of taxane family, namely paclitaxel (PTX), docetaxel (DTX) and cabazitaxel (CTX) have been approved by the US FDA for clinical use, with the first two being widely prescribed as front-line treatment options for many forms of cancers such as breast, ovarian and lung cancer [1,4–7]. CTX is the latest member of taxane family that has been approved for the treatment of hormone refractory prostate cancer [8]. Despite their widespread popularity, all three taxanes show very low solubility in water, thereby making development of effective formulations for medicinal use challenging. They are either formulated in a mixture of Cremophor EL/absolute ethanol or in Polysorbate 80, both of which are associated with serious side effects (hypersensitivity reactions, peripheral neurotoxicity, etc.) [9,10]. Patients receiving these drugs require premedication with steroids and benadryl. Application of nanomedicine in cancer field has led to the development and FDA approval of PTX-loaded human serum albumin nanoaggregates (Abraxane®) [11]. Although more drug can be given (240 mg/$m^2$ PTX for Abraxane vs 175 mg/$m^2$ PTX for paclitaxel), these nanoparticles are relatively 'large' (130 nm in diameter), and improvement in clinical efficacy is only marginal. A wide variety of newer PTX and DTX nanoformulations have been explored [12–14] such as NK105 [15] and Genexol-PM [16], which are under clinical development, and more recently CTX nanoformulations have been attempted [17,18]. Reports exist on encapsulation of PTX [19], DTX [20] and some third-generation taxoids (excluding CTX) [21] in poly(2-oxazoline)-based micelles. To the best of our knowledge, there is not a single polymer or nanoplatform that can stably encapsulate all the three FDA-approved members of taxane family with significant loading

Future Medicine part of fsg

capacity and efficiency. We have previously reported polyethylene glycol (PEG) and cholic acid (CA)-based micellar system $PEG^{5K}$-$CA_8$ telodendrimer (TD) [22] that can load PTX with very high capacity and efficiency. Here, we report the design, synthesis and characterization of a small set of structurally related amphiphilic polymers capable of nanoformulating all three members of the taxane family, with high efficiency, but lower hemolytic potential.

## Materials & methods

For synthesis and other experimental details, please see Supplementary Information file.

## Results

With the development of several nanocarriers based on liposomes, micelles, polymers, hydrogels etc., many hydrophobic cancer drugs can now be stably encapsulated and delivered site specifically to cancer site via active or passive targeting [14,23–27]. We have recently reported a robust micellar nanoparticle platform that can stably encapsulate a range of hydrophobic agents in the hydrophobic core [22,28–34]. This nanoplatform is assembled from amphiphilic TDs comprised of natural surfactant CA and dendritic lysines linked to a linear PEG, represented by the formula $PEG^{nK}$-$CA_y$ (where n = molecular weight in kilodaltons [K], y = number of CA units). $PEG^{5K}$-$CA_8$ (Figure 1), one of our most studied TD can stably encapsulate a range of cancer drugs including PTX, a taxane [22], and a number of other chemotherapeutic agents. TD-encapsulated PTX with almost 100% loading efficiency when the initial amount of PTX was less than 25 wt% of $PEG^{5K}$-$CA_8$ (20 mg/ml), with superior stability (longer than 6 months) and a size of 20–60 nm [22]. Though $PEG^{5K}$-$CA_8$ showed superior loading capability with PTX, it failed to do so with DTX and CTX (see Tables 3 & 5). Given that all three taxanes are structurally quite similar (Figure 1), this result is somewhat surprising. It underscores the importance of matching the right nanocarrier with the intended drug payload.

Versatility of our nanoplatform lies in its architecture that allows for easy structural modulation to meet the desired goal [35,36] such as substituting some CAs with organic moieties (OMs). We believe such modifications will enable us to generate novel TDs that are tailored toward specific drug or groups of drugs. Replacing four of the eight CAs in $PEG^{5K}$-$CA_8$ with OMs generated TDs (hybrid TDs), represented as $PEG^{5K}$-$OM_4$/$CA_4$ (Figure 2). We also developed structural analogs of $PEG^{5K}$-$CA_8$, where all the eight CAs were replaced with OMs (polymers designated as $PEG^{5K}$-$OM_8$) to examine the contribution of CA to drug loading. All the polymers were prepared according to our well-established published procedures [22,36].

### Characterization

Molecular weights of all the prepared polymers were measured with MALDI-TOF mass spectrometry. The molecular weights of the polymers (Table 1) matched closely with the theoretical values (Tables 1 & 2). The molecular weight distribution between the polymers and the corresponding starting PEG were almost identical (see representative examples in Supplementary Figure 3). Nuclear magnetic resonance (NMR) analysis was done to confirm grafting of cholane and OM on the PEG chain (Tables 1 & 2). Signals of PEG chain (3.6 ppm) and of CA methyl peaks at 0.66, 0.87 and 1.01 ppm, as previously used by our group [22,37], along with characteristic peaks of OM, were used for analysis (Supplementary Figure 4 for representative examples). Based on the average molecular weight (5000) of PEG chains, ratio of PEG protons to that of cholane and organic moieties was very close to the expected values, which indicated successful grafting. HPLC was used to assess the purity of the samples. Based on tert-butyloxycarbonyl (Boc)-protected starting material, newly prepared TDs showed chromatograms similar to Boc-$PEG^{5K}$-$NH_2$. Based on the heterogeneity of the starting material and samples very broad peak, it was difficult to judge degree of impurity of the final TD product (Supplementary Figure 5 for representative examples). The particle size of the micelles formed by self-assembly of the polymers in phosphate-buffered saline (PBS) is shown in Tables 1 & 2. Almost all the prepared hybrid polymers (Table 1) yielded particle sizes in the range of 7 to 32 nm with a narrow size distribution. Only TD 9 ($PEG^{5K}$-[Retinoic acid]$_4$/$CA_4$) has a minor portion of aggregates (2000 nm). Moreover, all the prepared hybrid TDs have good water solubility (up to at least 15 mg/ml, data not shown) with critical micelle concentration (CMC) values ranging between 1 and 6 μM, as determined by using pyrene as a hydrophobic probe (Supplementary Figure 6 for representative example). Compared with hybrid TDs, nanoparticles assembled from $PEG^{5K}$-$OM_8$-based polymers showed a much broader size distributions (Table 2) and several of them generated heterogenous populations of nanoparticles with different sizes. Only $PEG^{5K}$-$(Biotin)_8$, $PEG^{5K}$-$(Glycocholic\ acid)_8$ and $PEG^{5K}$-$(Chenodeoxycholic\ acid)_8$ yielded particle size distributions comparable to those produced by the hybrid polymers. Several of them (entry 16, 17, 21 and 22) became poorly soluble with higher ionic strength (<0.25 mg/ml in PBS), and were not evaluated further for CMC values. CMC values are

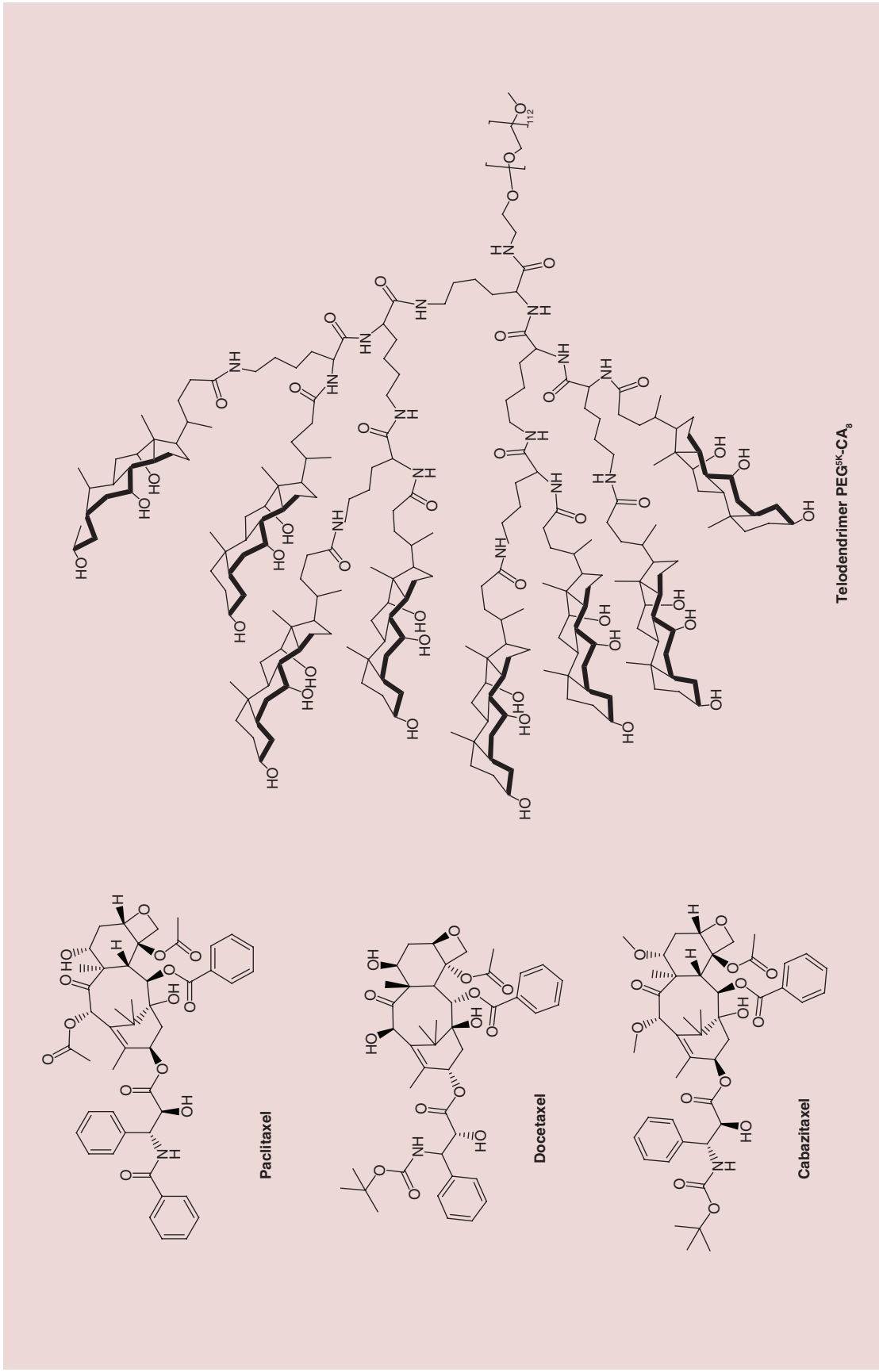


**Figure 1. Chemical structures of FDA-approved taxanes and $PEG^{5K}$-$CA_8$ TD.**

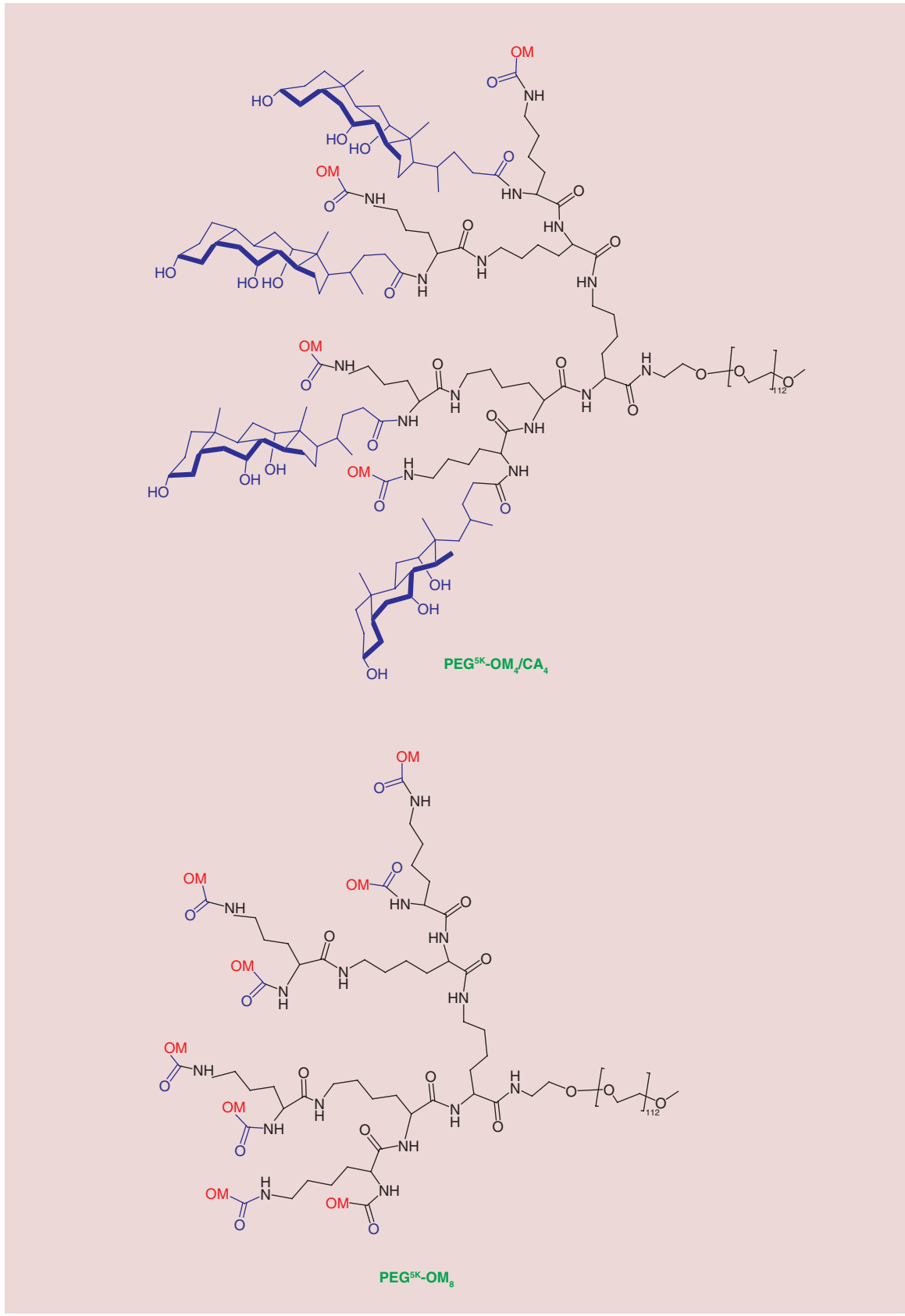


**Figure 2. Representative structures of the two types of amphiphilic polymers used in this study.**

Table 1. Characterization of micelles formed by hybrid telodendrimers (PEG$^{5K}$-OM$_4$/CA$_4$).

| Entry | OM | Polymer | Molecular. weight exp. (theo.) (Da) | NMR cholane:PEG:OM or cholane+OM:PEG obs (theo.) | CMC (μM) | Particle size (volume%, width) (nm) |
|---|---|---|---|---|---|---|
| 1 | Biotin (vitamin H) 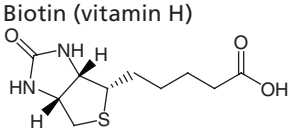 | PEG$^{5K}$-(Biotin)$_4$/CA$_4$ | 7984 (8416) | 1[†]:15.17 (1:12.44) | 3 | 11.2 (100, 7.13) |
| 2 | *trans*-cinnamic acid (used as flavoring agent) 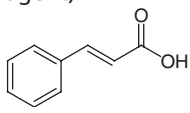 | PEG$^{5K}$-(Cinnamic acid)$_4$/CA$_4$ | 7758 (8033) | 1:15.27:0.42 (1:12.44:0.44[‡]) | 1 | 20.1 (100, 7.8) |
| 3 | Lauric acid (saturated fatty acid) 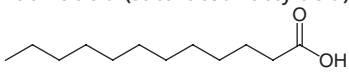 | PEG$^{5K}$-(Lauric acid)$_4$/CA$_4$ | 7919 (8241) | 1:11.28 (1[§]:9.33) | 3 | 20.8 (100, 32.7) |
| 4 | Linoleic acid (polyunsaturated fatty acid) 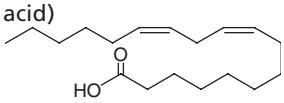 | PEG$^{5K}$-(Linoleic acid)$_4$/CA$_4$ | 8146 (8561) | 1:10.23 (1[¶]:9.33) | 1 | 31.2 (91.3, 21.4)/ 129.5 (8.7, 93.5) |
| 5 | Lipoic acid (cofactor) 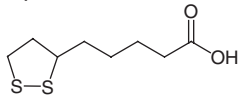 | PEG$^{5K}$-(Lipoic acid)$_4$/CA$_4$ | 7819 (8265) | 1:13.65:0.19 (1:12.44:0.22[#]) | 2 | 11.8 (100, 10.3) |
| 6 | Nicotinic acid (vitamin B3) 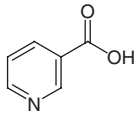 | PEG$^{5K}$-(Nicotinic acid)$_4$/CA$_4$ | 7788 (7931) | 1[††]:16.75 (1:12.44) | 4 | 10.6 (100, 6.37) |
| 7 | Octanoic acid (saturated fatty acid) 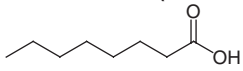 | PEG$^{5K}$-(Octanoic acid)$_4$/CA$_4$ | 7548 (8016) | 1:11.46 (1[‡‡]:9.33) | 2 | 10.7 (100, 11.6) |
| 8 | Oleic acid (mono unsaturated fatty acid) 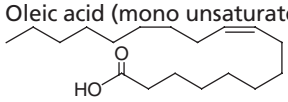 | PEG$^{5K}$-(Oleic acid)$_4$/CA$_4$ | 8472 (8569) | 1:11.86 (1[§§]:9.33) | 3 | 15.9 (100, 22.7) |
| 9 | Retinoic acid (vitamin A metabolite) 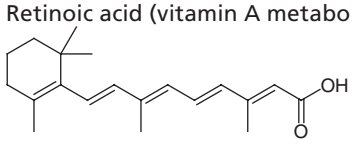 | PEG$^{5K}$-(Retinoic acid)$_4$/CA$_4$ | 7961 (8641) | 1:9.42 (1[¶¶]:7.47) | 6 | 7.9 (95.7, 7.69)/ 2048 (4.3, 720) |
| 10 | Sorbic acid (food preservative) 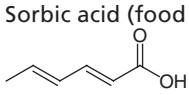 | PEG$^{5K}$-(Sorbic acid)$_4$/CA$_4$ | 7620 (7891) | 1:11.09 (1[##]:12.44) | 4 | 6.9 (89, 4.7)/ 32.1 (11, 15.9) |

[†]Biotin peaks either overlap with backbone or not strongly differentiable from background.
[‡]4H of cinnamic between 7.3 and 7.5 ppm.
[§]Lauric methyl along with cholane methyl.
[¶]Linoleic methyl along with cholane methyl.
[#]2H of lipoic between 3.12 and 3.18 ppm.
[††]1H proton peaks from nicotinic present but not strongly differentiable from background. Only cholane peak used.
[‡‡]Octanoic methyl along with cholane methyl.
[§§]Oleic methyl peak along with cholane methyl.
[¶¶]Two methyl present on quaternary carbon in retinoic cyclic ring along with cholane.
[##]Vinyl proton of sorbic present but not strongly differentiable from background. Only cholane peak used.
CA: Cholic acid; CMC: Critical micelle concentration; exp.: Experimental; NMR: Nuclear magnetic resonance; obs.: Observed; OM: Organic moiety; PEG: Polyethylene glycol; theo.: Theoretical.

reported in Table 2, for the $PEG^{5K}$-$OM_8$ polymers with solubility ≥2 mg/ml. CMC values were found to be in the range of 2–22 μM. Based on the solubility (at least 15 mg/ml, data not shown), low CMC value and size distribution, only the following, among the $PEG^{5K}$-$OM_8$ group, were selected for further studies: $PEG^{5K}$-$(Biotin)_8$, $PEG^{5K}$-$(Glycocholic\ acid)_8$, $PEG^{5K}$-$(Chenodeoxycholic\ acid)_8$ and $PEG^{5K}$-$(Nicotinic\ acid)_8$. We selected 14 polymers (four $PEG^{5K}$-$OM_8$ and ten hybrid TDs) to determine particle size variation as a function of polymer concentration (0.5 and 5 mg/ml). Except for polymers 8 and 11 that generated significant size variations at the two different concentrations, the remaining polymers showed nearly similar size distribution (Supplementary Table 1).

## Hemolysis

Hemolysis induced by hybrid TDs and selected $PEG^{5K}$-$OM_8$ polymers were examined to gain insight into their hematocompatibility. Hemolysis was detected through spectrophotometric measurement of the hemoglobin present in the supernatant of red blood cells (RBCs) treated with the micellar nanoparticles. Previously, we have shown dose-dependent RBC lysis from standard TD $PEG^{5K}$-$CA_8$. Hemolysis increased from 9.0 to 16.3% when the concentration of $PEG^{5K}$-$CA_8$ was increased from 0.2 to 1.0 mg/ml, respectively [38]. For the current set of polymers, hemolytic studies were performed at concentrations of 0.2 and 2 mg/ml (expected blood levels during therapy). Figure 3 shows the observed hemolytic activity from the hybrid TDs and $PEG^{5K}$-$OM_8$ polymers. At 0.2 mg/ml, most of the polymers showed no hemolytic activity except $PEG^{5K}$-$(Glycocholic\ acid)_8$ polymer (81.9%). Hemolysis from $PEG^{5K}$-$(Octanoic\ acid)_4/CA_4$ and $PEG^{5K}$-$(Retinoic\ acid)_4/CA_4$ were significantly lower (4.0 and 5.5%, respectively). At higher polymer concentration (2 mg/ml), except for $PEG^{5K}$-$(Retinoic\ acid)_4/CA_4$ that showed hemolysis in double digits (16.2%) and $PEG^{5K}$-$(Glycocholic\ acid)_8$ that showed even higher hemolysis (90.9%), most of the hybrid TDs and $PEG^{5K}$-$OM_8$ were either devoid of hemolytic activity or only induced minimal hemolysis (2.7, 3.4 and 4.7% for lauric-, lipoic- and octanoic-based hybrid TDs, respectively, and 1.9% for $PEG^{5K}$-$[Biotin]_8$). The high hemolytic activity of $PEG^{5K}$-$(Retinoic\ acid)_4/CA_4$ and $PEG^{5K}$-$(Glycocholic\ acid)_8$ is of concern, but can probably be mitigated by introducing disulfide cross-links in the hydrophobic core as previously reported for our standard TD [38]. Hemolytic activity was also evaluated at 4 mg/ml for localized concentrations effect. Results were quite similar to 2 mg/ml, with marginally increased hemolysis from lauric- and octanoic-based hybrid TDs (Supplementary Figure 7).

## *In vitro* cytotoxicity

Empty nanoparticles assembled from hybrid TDs were evaluated for cytotoxicity against human breast cancer cells MDA-MB-231 using an MTS assay. As shown in Figure 4, the nanocarriers did not exhibit detectable cytotoxicity up to at least 2 mg/ml for incubation over 48 or 72 h, except for $PEG^{5K}$-$(Glycocholic\ acid)_8$, which showed some toxicity at the 72 h time point. When examined at even much higher levels (4 and 6 mg/ml), most of the polymers still lacked any significant toxicity. Notable exceptions are linoleic acid and retinoic hybrid, with less than 50% viability at 48 and 72 h, and $PEG^{5K}$-$Nicotinic_8$ at 72 h. Viability for $PEG^{5K}$-$(Glycocholic\ acid)_8$ was about 50% at 72 h. Lack of significant cytotoxicity from most of these micelles indicates their potential usage as drug carrier for nanoformulation.

## Drug loading for DTX, CTX & PTX

Over the past several years, we have successfully loaded a number of hydrophobic drugs (PTX, doxoruicin, vincristine, daunorubicin, etc.) in our standard nanomicelles assembled from $PEG^{5K}$-$CA_8$ and these nanoformulations were proven to be efficacious in several xenograft models [22,28,30,32,39,40]. However, we have also found that $PEG^{5K}$-$CA_8$ does not work for all hydrophobic drugs such as DTX (Table 3), CTX (Table 5) and SN-38 (data not shown). In order to show versatility and flexibility of our nanomicelles, we evaluated a small set of polymers for their ability to encapsulate DTX (Tables 3 & 4) and CTX (Tables 5 & 6).

As shown in Table 3, loading efficiency of the standard TD $PEG^{5K}$-$CA_8$ for DTX at 10% drug:polymer ratio (w/w) was found to be 69%. At the very same drug:polymer ratio, six different hybrid TDs were found to have higher drug-loading efficiencies than that of $PEG^{5K}$-$CA_8$ (polymers 1, 2, 5, 6, 7 and 10). Among the $PEG^{5K}$-$CA_8$ class, $PEG^{5K}$-$(Glycocholic\ acid)_8$ has better loading efficiency than that of the standard TD. Other than $PEG^{5K}$-$(Octanoic\ acid)_4/CA_4$ (polymer 7), all other favorable candidates had particle sizes less than 20 nm with narrow size distribution. Moreover three of them, namely polymer 2 ($PEG^{5K}$-$(Cinnamic\ acid)_4/CA_4$); polymer 5 ($PEG^{5K}$-$(Lipoic\ acid)_4/CA_4$) and polymer 10 ($PEG^{5K}$-$(Sorbic\ acid)_4/CA_4$) encapsulated DTX with 100% efficiency. These three polymers were selected for loading at a higher drug concentration (Table 4). At DTX loading of 3/15-mg polymer, both 2 and 5 still retained the high drug-loading efficiency (93 and 87%, respectively), but loading efficiency of 10 was found to drop to 57%. Based on the DTX screening, we identified two polymers, 2 and 5, that can stably encapsulate DTX with significant loading capacity (nearly 20%

Table 2. Characterization of micelles formed by polymers ($PEG^{5K}$-$OM_8$).

| Entry | Polymer | Molecular weight exp. (theo.) (Da) | NMR† OM:PEG obs (theo.) | CMC (μM) | Particle size (volume%, width) (nm) |
|---|---|---|---|---|---|
| 11 | $PEG^{5K}$-$(Biotin)_8$ | 7769 (7760) | NC‡ | 2 | 12.5 (100, 10.8) |
| 12 | $PEG^{5K}$-$(Chenodeoxycholic\ acid)_8$ 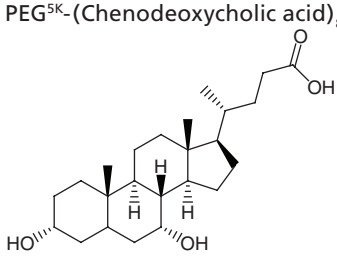 | 8600 (8946) | 1:5.99 (1:6.22) | 2 | 32.5 (100, 25.1) |
| 13 | $PEG^{5K}$-$(Cinnamic\ acid)_8$ | 6994 (6991) | 1:17.78 (1:14) | 22 | 17.2 (97.5, 28.9)/5810 (2.5, 973) |
| 14 | $PEG^{5K}$-$(Glycocholic\ acid)_8$ 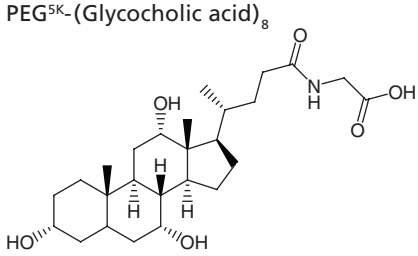 | 9472 (9531) | 1:7.01 (1:6.22) | 1 | 18.1 (100, 8.4) |
| 15 | $PEG^{5K}$-$(Lauric\ acid)_8$ | 7445 (7409) | 1:5.62 (1§:3.5) | 13 | 10.3 (9.7, 2.3)/27.8 (90.3, 31) |
| 16 | $PEG^{5K}$-$(Linoleic\ acid)_8$ | N.O. (8050) | 1:15.79 (1:18.67) | ND | 19.1 (97.4, 28.9)/5780 (2.6, 3170)‡‡ |
| 17 | $PEG^{5K}$-$(Lipoic\ acid)_8$ | N.O. (7457) | N.O. | ND | Wide range of distribution from 21 to 5700 nm‡‡ |
| 18 | $PEG^{5K}$-$(Nicotinic\ acid)_8$ | 6867 (6791) | NC¶ | 3 | 1 (32.3, 0.3)/75.3 (56.3, 81)/ 377 (11.4, 229) |
| 19 | $PEG^{5K}$-$(Octanoic\ acid)_8$ | 6915 (6960) | 1:9.39 (1#:7) | 3 | 15.3 (12.3, 5.2)/44.7 (82.7, 49.1)/ 5970 (5, 676) |
| 20 | $PEG^{5K}$-$(Oleic\ acid)_8$ | 7944 (8066) | 1:21.85 (1:18.67) | 3 | 40.9 (89.4, 43.5)/1249 (3.3, 527)/ 5740 (7.3, 1096) |
| 21 | $PEG^{5K}$-$(Retinoic\ acid)_8$ | 7800 (8209) | 1:11.66 (1:9.33) | ND | 28 (89.9, 32.7)/456 (5.7, 298.7)/ 1842 (4.4, 1644)‡‡ |
| 22 | $PEG^{5K}$-$(Sorbic\ acid)_8$ | 6396 (6703) | NC†† | ND | 25.3 (86.2, 33.4)/5810 (13.8, 958)‡‡ |

†Peaks used that are different from Table 1 are summarized below.
‡NC: Not calculated. Biotin peaks either overlap with backbone or not strongly differentiable from background.
§8, $CH_2$: 1.07–01.46 ppm.
¶1H proton peaks from nicotinic present but not strongly differentiable from background.
#4, $CH_2$ peak around 1.29 ppm.
††Vinyl proton of sorbic present but not strongly differentiable from background.
‡‡Measured at around 0.2 mg/ml.
CMC: Critical micelle concentration; exp.: Experimental; ND: Not determined; NMR: Nuclear magnetic resonance; obs.: Observed; OM: Organic moiety; PEG: Polyethylene glycol; theo.: Theoretical.

w/w). Nanoformulations were considered stable if they did not form a visible precipitate after 48-h storage at 4°C and if they maintained nearly the same particle size (monitored by dynamic light scattering [DLS], data not shown).

CTX, another member of taxane family and recently approved for the treatment of prostate cancer was screened next. Compared with DTX, CTX had a better drug loading (Table 5) in standard TD $PEG^{5K}$-$CA_8$ (79% at 2.0 mg of CTX compared with 69% at 1.5 mg of DTX per 15 mg of polymer). Despite better loading of CTX than DTX by $PEG^{5K}$-$CA_8$, broader size distribution of the final nanoparticles was observed in CTX formulation. Compared with $PEG^{5K}$-$CA_8$, four hybrid TDs, namely 2, 4, 5 and 7, showed better loading efficiency while $PEG^{5K}$-$(Oleic\ acid)_4$/$CA_4$ (poly-

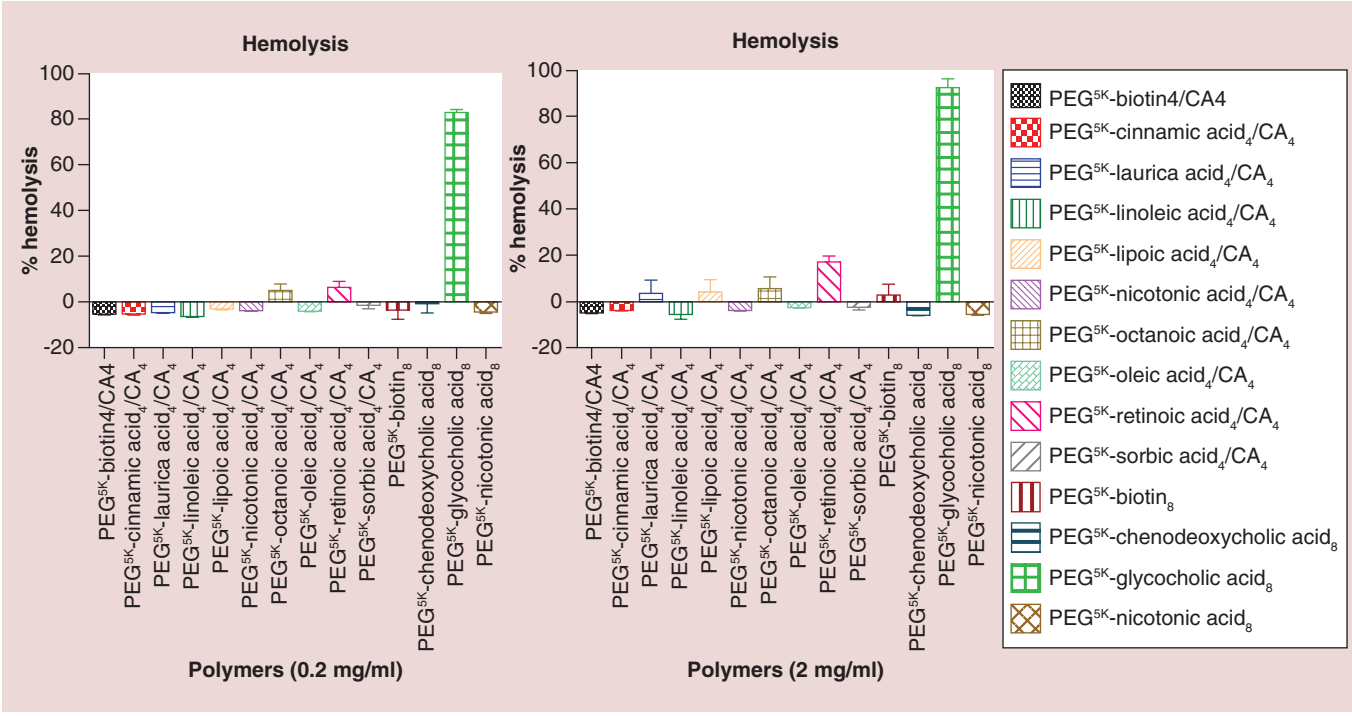


**Figure 3. *In vitro* red blood cell (RBC) lysis from selected polymers. RBC incubation with Triton-100 (2%) and PBS were used as the positive and negative controls, respectively. Values reported are the mean ± SD for triplicate samples.**

mer 8) showed similar loading efficiency. On the other hand, none of the PEG$^{5K}$-OM$_8$ polymers showed better drug loading than PEG$^{5K}$-CA$_8$. PEG$^{5K}$-(Cinnamic acid)$_4$/CA$_4$ (polymer 2) and PEG$^{5K}$-(Linoleic acid)$_4$/CA$_4$ (polymer 4), both of which showed 100% loading efficiency, were tested further for higher drug loading. Both of these hybrid TDs were found to retain nearly 100% loading efficiency at 3 mg of drug and 15 mg of polymer (Table 6). Based on CTX screening, two polymers with significant loading capacity (nearly 20% w/w) were identified and loading was even better when compared with the results of DTX. For representative DLS data on drug-loaded samples (Tables 3 & 5), see Supplementary Figure 8.

PEG$^{5K}$-(Cinnamic acid)$_4$/CA$_4$, PEG$^{5K}$-(Linoleic acid)$_4$/CA$_4$ and PEG$^{5K}$-(lipoic acid)$_4$/CA$_4$ were also evaluated for PTX encapsulation. While PEG$^{5K}$-(Linoleic acid)$_4$/CA$_4$ showed 100% loading efficiency

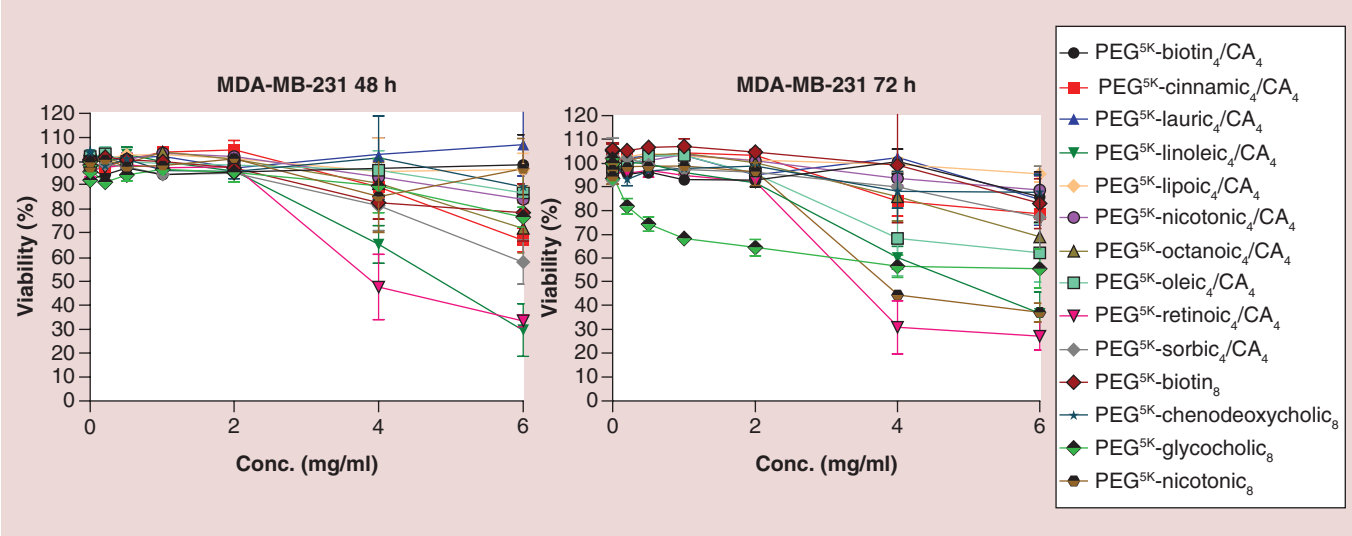


**Figure 4. The cytotoxicity of empty hybrid TDs against MDA-MB-231 breast cancer cells. Values reported are the mean ± SD for triplicate samples.**

Table 3. Docetaxel loading (1.5 mg/15 mg polymer, n = 1).

| Polymer | Particle size (volume%, width) (nm) | Drug/polymer (w/w) (%) | Loading efficiency (%) |
|---|---|---|---|
| $PEG^{5K}$-$CA_8$ | 13.3 (100, 8.01) | 10 | 69 |
| 1 | 10.5 (100, 7.91) | 10 | 74 |
| 2 | 12.9 (100, 7.88) | 10 | 100 |
| 3 | 19.6 (95, 16.67)/295.4 (5, 312) | 10 | 0 |
| 4 | 9.35 (100, 7.78) | 10 | Precipitated |
| 5 | 11.8 (100, 10.3) | 10 | 100 |
| 6 | 10.8 (100, 8.3) | 10 | 77 |
| 7 | 13.6 (95.1, 12.53)/122.8 (4.9, 206.5) | 10 | 90 |
| 8 | 13 (100, 10.33) | 10 | 2 |
| 9 | 12.4 (93.9, 9.65)/338 (6.1, 226.5) | 10 | 61 |
| 10 | 12.3 (100, 7.67) | 10 | 100 |
| 11 | 11 (95.9, 9.42)/1087 (4.1, 2586) | 10 | 21 |
| 12 | 16.1 (100, 9.07) | 10 | 1 |
| 14 | 19.7 (100, 8.88) | 10 | 85 |
| 18 | 6.5 (19.8, 2)/11.3 (24.2, 5.4)/33.6 (50.5, 27.8)/173.6 (5.5, 109.9) | 10 | 18 |

PEG: Polyethylene glycol; CA: Cholic acid.

only at 5% w/w, $PEG^{5K}$-(Cinnamic acid)$_4$/$CA_4$ and $PEG^{5K}$-(lipoic acid)$_4$/$CA_4$ showed 100% efficiency up to 15% w/w and 20% w/w loading, respectively (Supplementary Table 2 for particle size distribution).

## Discussion

As the amphiphilic TDs are prepared by step-wise peptide-synthesis method, we can easily introduce different linkers, amphiphilic building blocks or OM to the termini of the PEG-oligolysine (or other diaminocarboxylic acid) dendrimer [35]. Here, we focused our effort on developing TDs that can encapsulate all three taxanes: PTX, DTX and CTX. To minimize toxicity from these newer TDs, we selected only those OMs that are either produced endogenously, consumed by human as part of their diet, or are FDA-approved drugs or food additives. Chemical structures of simple aliphatic or aromatic OMs used to prepare different hybrid TDs are shown in Table 1. For our initial study, we focused on small set of saturated and unsaturated fatty acids (entry 3, 4, 7 and 8), cyclic vitamins (entry 1, 6 and 9, with 1 and 6, also being heterocyclic compounds), a flavoring agent and food preservative (entry 2 and 10, respectively) and lastly a cofactor (entry 5, which is also heterocyclic compound). We also included natural surfactants chenodeoxycholic acid and glycocholic acid as an alternative to CA (Table 2, entry 12 and 14) for the polymer class $PEG^{5K}$-$OM_8$. Compared with majority of $PEG^{5K}$-$OM_8$, $PEG^{5K}$-(OM)$_4$/$CA_4$ TDs displayed narrower size distribution, lower CMC values and better aqueous solubility. Our previously reported standard TD $PEG^{5K}$-$CA_8$ also has CMC value in the same range (5.3 μM) [28], indicating that substitution of four CAs with other organic blocks has minor effects on the CMC values. Hematocompatibility is necessary for clinical translation of polymer-based drug carriers. Amphiphilic polymers have the potential to cause disruption of the plasma membrane, particularly of RBCs. When tested for their hemolytic potential, hybrid

Table 4. Docetaxel loading (3 mg/15 mg polymer; mean ± SD, n = 3).

| Polymer | Particle size (volume%, width) (nm) | 3-mg DTX | |
|---|---|---|---|
| | | Drug/polymer (w/w)(%) | Loading efficiency(%) |
| 2 | 27.7 (100, 16.7) | 20 | 93 ± 2.9 |
| 5 | 27.3 (100, 22.9) | 20 | 87 ± 3.2 |
| 10 | 140.5 (39.5, 73.9)/443 (60.5, 235.9) | 20 | 57 ± 1.4 |

DTX: Docetaxel; SD: Standard deviation.

Table 5. Cabazitaxel loading (2.0 mg/15 mg polymer, n = 1).

| Polymer | Particle size (volume%, width) (nm) | Drug/polymer (w/w) (%) | Loading efficiency (%) |
|---|---|---|---|
| $PEG^{5K}$-$CA_8$ | 15.8 (96.2, 33)/348 (3.8, 1983) | 13.35 | 79 |
| 1 | 23.9 (100, 28.9) | 13.35 | 57 |
| 2 | 15.9 (95.3, 7.13)/222.9 (4.7, 304) | 13.35 | 100 |
| 3 | 16.9 (15.4, 4.2)/49.8 (84.6, 74.4) | 13.35 | 38 |
| 4 | 20.73 (100, 12.15) | 13.35 | 100 |
| 5 | 0.99 (31, 0.22)/15.38 (69, 11.87) | 13.35 | 89 |
| 6 | 11.87 (100, 10.6) | 13.35 | 41 |
| 7 | 18.0 (100, 14.4) | 13.35 | 82 |
| 8 | 25.27 (100, 69.9) | 13.35 | 80 |
| 9 | 23.3 (100, 24.0) | 13.35 | 66 |
| 10 | 16.2 (100, 10.0) | 13.35 | 74 |
| 11 | 27.9 (95.3, 56.1)/1399 (4.7, 1193) | 13.35 | 31 |
| 12 | 23.98 (100, 27.6) | 13.35 | 70 |
| 14 | 0.96 (100, 0.21) | 13.35 | 55 |
| 18 | 84.4 (94.6, 70)/396 (5.4, 229.4) | 13.35 | 69 |

PEG: Polyethylene glycol; CA: Cholic acid.

TD (except retinoic acid one), behaved much more like control, PBS, at 2 mg/ml concentration indicating their usefulness as drug carriers. Moreover, lack of any apparent cytotoxicity from majority of these TDs further reinforces their nanocarrier potential. When tested for their drug-loading potential, several TDs outweighed $PEG^{5K}$-$CA_8$ in terms of loading efficiency (Tables 3 & 5). Of the 15 TDs ($PEG^{5K}$-$(OM)_4/CA_4$ and $PEG^{5K}$-$OM_8$) evaluated for DTX and CTX loading, two from each group were found to have significant loading capacity. Loading efficiency was nearly 100% when the initial amount of DTX or CTX used was less than 20 wt% of the polymer, a result matching to our prior observation with PTX loading by $PEG^{5K}$-$CA_8$. Nanoformulations were stable with narrow size distribution. These data indicate that CA, compared with other OMs, has a unique physicochemical property such that its presence at 50% level at the dendron is able to maintain the stability, monodisperse property and small size (<50 nm) of the nanocarrier, and to stably encapsulate hydrophobic drugs. It appears that the amphiphilic nature of the rigid, disc-shaped tetracyclic CA molecule, with three hydroxyl groups facing one side and hydrophobic ring surfaces facing the other, may allow the CAs to assemble as a stable barrier between the hydrophilic PEG corona and hydrophobic core of the nanocarrier. On special note, based on our result so far, $PEG^{5K}$-$(Cinnamic\ acid)_4/CA_4$ seems to be the best TD of the lot as it stably encapsulated all members of taxane family with significant loading. Also, our data suggest hybrid system to be much more robust and efficient when compared with $PEG^{5K}$-$OM_8$, again signifying the importance of CA moiety in the scaffold. In summary, we have generated a small set of robust TDs that can be synthesized easily. We are currently testing these nanoformulations in various mouse models for their *in vivo* therapeutic efficacy and toxicity. We are also screening these polymers and other new hybrid TDs for their capacity to load other hydrophobic drugs that have poor loading capacity with our standard polymer. We believe that this systematic experimental approach will enable us

Table 6. Cabazitaxel loading (3 mg/15 mg polymer; mean ± SD, n = 3).

| Polymer | Particle size (volume%, width) (nm) | 3-mg CTX | |
|---|---|---|---|
| | | Drug/polymer (w/w) (%) | Loading efficiency (%) |
| 2 | 22 (100, 11.3) | 20 | 93 ± 4.9 |
| 4 | 37.5 (100, 29.9) | 20 | 98 ± 3.4 |

CTX: Cabazitaxel; SD: Standard deviation.

to tailor specific TDs for nanoformulation of many current and future toxic drugs, thus enhancing their therapeutic index and efficacy.

## Conclusion

The modular CA-based micellar nanocarrier platform allows systematic incorporation of additional organic moieties into the amphiphilic polymer, such that the resulting hybrid TDs can be tailored for a wide range of otherwise hard to nanoformulate hydrophobic drugs. Here, we have shown their utility in successful nanoformulation of approved taxane with significant loading capacity.

### Supplementary data

To view the supplementary data that accompany this paper please visit the journal website at: www.futuremedicine.com/doi/full/10.2217/nnm-2017-0361

### Financial & competing interests disclosure

The authors thank NIH for the funding support: 3R01CA115483, 1U01CA198880-01 to KS Lam and 5R01CA199668 to Y Li. G Bharadwaj, Y Li and KS Lam are the inventors of a pending patent on hybrid TDs (US Patent Application no. 62/395,237). KS Lam is the founding scientist of LamnoTherapeutics, Inc., which plan to develop the nanotherapeutics described in the manuscript. The authors have no other relevant affiliations or financial involvement with any organization or entity with a financial interest in or financial conflict with the subject matter or materials discussed in the manuscript apart from those disclosed.

No writing assistance was utilized in the production of this manuscript.

### Ethical conduct of research

All animals were kept under pathogen-free conditions according to AAALAC guidelines. All animal experiments were performed in compliance with institutional guidelines and according to protocol approved by the Animal Use and Care Administrative Advisory Committee at the University of California, Davis. The authors state that they have obtained appropriate institutional review board approval or have followed the principles outlined in the Declaration of Helsinki for all human or animal experimental investigations.

### Executive summary

**Synthesis of $PEG^{5K}$-$OM_4/CA_4$ & $PEG^{5K}$-$OM_8$**

- Solution-phase peptide synthesis was used to synthesize 22 new polymers.

**Physicochemical properties**

- Molecular weights of prepared polymers match with theoretical values. NMR reveals successful grafting of cholane and organic moiety. Hybrid telodendrimers have narrow size distribution, similar CMC values and better aqueous solubility compared with majority of $PEG^{5K}$-$OM_8$.

**Hemolysis & *in vitro* toxicity**

- Out of the 14 polymers tested for hemolytic potential, 12 of them showed minimal or no hemolysis at 2 mg/ml concentration.
- When tested for potential cytotoxicity, almost all the polymers tested (up to 2 mg/ml) showed no toxicity up to 72 h.

**Drug loading**

- $PEG^{5K}$-(Cinnamic acid)$_4$/$CA_4$ and $PEG^{5K}$-(Lipoic acid)$_4$/$CA_4$ showed nearly 100% loading for docetaxel (3 mg drug/15 mg polymer).
- $PEG^{5K}$-(Cinnamic acid)$_4$/$CA_4$ and $PEG^{5K}$-(Linoleic acid)$_4$/$CA_4$ showed nearly 100% loading for cabazitaxel (3 mg drug/15 mg polymer).
- $PEG^{5K}$-(Cinnamic acid)$_4$/$CA_4$ also showed 100% loading for paclitaxel (2.25 mg drug/15 mg polymer).

## References

1 Rowinsky EK. The development and clinical utility of the taxane class of antimicrotubule chemotherapy agents. *Annu. Rev. Med.* 48, 353–374 (1997).

2 Yared JA, Tkaczuk KH. Update on taxane development: new analogs and new formulations. *Drug Des. Devel. Ther.* 6, 371–384 (2012).

3 Wang Y-F, Shi Q-W, Dong M, Kiyota H, Gu Y-C, Cong B. Natural taxanes: developments since 1828. *Chem. Rev.* 111(12), 7652–7709 (2011).

4 De Weger VA, Beijnen JH, Schellens JH. Cellular and clinical pharmacology of the taxanes docetaxel and paclitaxel – a review. *Anti-Cancer Drugs* 25(5), 488–494 (2014).

5 Bedard PL, Di Leo A, Piccart-Gebhart MJ. Taxanes: optimizing adjuvant chemotherapy for early-stage breast cancer. *Nat. Rev. Clin. Oncol.* 7(1), 22–36 (2010).

6 Chu Q, Vincent M, Logan D, Mackay JA, Evans WK. Taxanes as first-line therapy for advanced non-small cell lung cancer: a systematic review and practice guideline. *Lung Cancer* 50(3), 355–374 (2005).

7 Guastalla Iii JP, Dieras V. The taxanes: toxicity and quality of life considerations in advanced ovarian cancer. *Br. J. Cancer* 89(Suppl 3), S16–S22 (2003).

8 Bishr M, Saad F. Overview of the latest treatments for castration-resistant prostate cancer. *Nat. Rev. Urol.* 10(9), 522–528 (2013).

9 Reddy LH, Bazile D. Drug delivery design for intravenous route with integrated physicochemistry, pharmacokinetics and pharmacodynamics: illustration with the case of taxane therapeutics. *Adv. Drug Del. Rev.* 71, 34–57 (2014).

10 Joerger M. Treatment regimens of classical and newer taxanes. *Cancer Chemother. Pharmacol.* 77(2), 221–233 (2016).

11 Gradishar WJ. Albumin-bound paclitaxel: a next-generation taxane. *Expert Opin. Pharmacother.* 7(8), 1041–1053 (2006).

12 Jäger E, Jäger A, Chytil P *et al.* Combination chemotherapy using core-shell nanoparticles through the self-assembly of HPMA-based copolymers and degradable polyester. *J. Control. Release* 165(2), 153–161 (2013).

13 Bushman J, Vaughan A, Sheihet L, Zhang Z, Costache M, Kohn J. Functionalized nanospheres for targeted delivery of paclitaxel. *J. Control. Release* 171(3), 315–321 (2013).

14 Wang AZ, Langer R, Farokhzad OC. Nanoparticle delivery of cancer drugs. *Annu. Rev. Med.* 63, 185–198 (2012).

15 Kato K, Chin K, Yoshikawa T *et al.* Phase II study of NK105, a paclitaxel-incorporating micellar nanoparticle, for previously treated advanced or recurrent gastric cancer. *Invest. New Drugs* 30(4), 1621–1627 (2012).

16 Lee KS, Chung HC, Im SA *et al.* Multicenter Phase II trial of Genexol-PM, a cremophor-free, polymeric micelle formulation of paclitaxel, in patients with metastatic breast cancer. *Breast Cancer Res. Treat.* 108(2), 241–250 (2008).

17 Bensaid F, Thillaye Du Boullay O, Amgoune A *et al.* Y-shaped mPEG-PLA cabazitaxel conjugates: well-controlled synthesis by organocatalytic approach and self-assembly into interface drug-loaded core-corona nanoparticles. *Biomacromolecules* 14(4), 1189–1198 (2013).

18 Zhou G, Jin X, Zhu P *et al.* Human serum albumin nanoparticles as a novel delivery system for cabazitaxel. *Anticancer Res.* 36(4), 1649–1656 (2016).

19 Luxenhofer R, Schulz A, Roques C *et al.* Doubly amphiphilic poly(2-oxazoline)s as high-capacity delivery systems for hydrophobic drugs. *Biomaterials* 31(18), 4972–4979 (2010).

20 Han Y, He Z, Schulz A *et al.* Synergistic combinations of multiple chemotherapeutic agents in high capacity poly(2-oxazoline) micelles. *Mol. Pharm.* 9(8), 2302–2313 (2012).

21 He Z, Schulz A, Wan X *et al.* Poly(2-oxazoline) based micelles with high capacity for 3rd generation taxoids: preparation, *in vitro* and *in vivo* evaluation. *J. Control. Release* 208, 67–75 (2015).

22 Xiao K, Luo J, Fowler WL *et al.* A self-assembling nanoparticle for paclitaxel delivery in ovarian cancer. *Biomaterials* 30(30), 6006–6016 (2009).

23 Davis ME, Chen Z, Shin DM. Nanoparticle therapeutics: an emerging treatment modality for cancer. *Nat. Rev. Drug Discov.* 7(9), 771–782 (2008).

24 Xu S, Olenyuk BZ, Okamoto CT, Hamm-Alvarez SF. Targeting receptor-mediated endocytotic pathways with nanoparticles: rationale and advances. *Adv. Drug Deliv. Rev.* 65(1), 121–138 (2013).

25 Markman JL, Rekechenetskiy A, Holler E, Ljubimova JY. Nanomedicine therapeutic approaches to overcome cancer drug resistance. *Adv. Drug Deliv. Rev.* 65(13–14), 1866–1879 (2013).

26 Kamaly N, Xiao Z, Valencia PM, Radovic-Moreno AF, Farokhzad OC. Targeted polymeric therapeutic nanoparticles: design, development and clinical translation. *Chem. Soc. Rev.* 41(7), 2971–3010 (2012).

27 Iyer AK, Khaled G, Fang J, Maeda H. Exploiting the enhanced permeability and retention effect for tumor targeting. *Drug Disc. Today Targets* 11(17–18), 812–818 (2006).

28 Luo J, Xiao K, Li Y *et al.* Well-defined, size-tunable, multifunctional micelles for efficient paclitaxel delivery for cancer treatment. *Bioconjugate Chem.* 21(7), 1216–1224 (2010).

29 Xiao K, Luo J, Li Y, Lee JS, Fung G, Lam KS. PEG-oligocholic acid telodendrimer micelles for the targeted delivery of doxorubicin to B-cell lymphoma. *J. Control. Release* 155(2), 272–281 (2011).

30 Kato J, Li Y, Xiao K *et al.* Disulfide cross-linked micelles for the targeted delivery of vincristine to B-cell lymphoma. *Mol. Pharm.* 9(6), 1727–1735 (2012).

31 Lin TY, Zhang H, Luo J *et al.* Multifunctional targeting micelle nanocarriers with both imaging and therapeutic potential for bladder cancer. *Int. J. Nanomed.* 7, 2793–2804 (2012).

32 Zhang H, Li Y, Lin TY *et al.* Nanomicelle formulation modifies the pharmacokinetic profiles and cardiac toxicity of daunorubicin. *Nanomedicine* 9(12), 1807–1820 (2014).

33 Xiao K, Li Y-P, Wang C *et al.* Disulfide cross-linked micelles of novel HDAC inhibitor thailandepsin A for the treatment of breast cancer. *Biomaterials* 67, 183–193 (2015).

34 Lin TY, Li YP, Zhang HY *et al.* Tumor-targeting multifunctional micelles for imaging and chemotherapy of advanced bladder cancer. *Nanomedicine* 8(8), 1239–1251 (2013).

35 Shi C, Guo D, Xiao K, Wang X, Wang L, Luo J. A drug-specific nanocarrier design for efficient anticancer therapy. *Nat. Commun.* 6, 7449 (2015).

36 Li Y, Lin T-Y, Luo Y *et al.* A smart and versatile theranostic nanomedicine platform based on nanoporphyrin. *Nat. Commun.* 5, 4712 (2014).

37 Li Y, Xiao K, Luo J, Lee J, Pan S, Lam KS. A novel size-tunable nanocarrier system for targeted anticancer drug delivery. *J. Control. Release* 144(3), 314–323 (2010).

38 Li Y, Xiao K, Luo J *et al.* Well-defined, reversible disulfide cross-linked micelles for on-demand paclitaxel delivery. *Biomaterials* 32(27), 6633–6645 (2011).

39 Xiao K, Li Y, Lee JS *et al.* "OA02" peptide facilitates the precise targeting of paclitaxel-loaded micellar nanoparticles to ovarian cancer *in vivo*. *Cancer Res.* 72(8), 2100–2110 (2012).

40 Kenyon NJ, Bratt JM, Lee J *et al.* Self-assembling nanoparticles containing dexamethasone as a novel therapy in allergic airways inflammation. *PLoS ONE* 8(10), e77730 (2013).